Segmental Strain for Myocardial Scar Detection in Acute Infarcts and Follow-Up CMR Using Non-Contrast Cine Images

Malgorzata Polacin (Malgorzata.Polacin@usz.ch)
University Hospital Zurich: UniversitatsSpital Zurich
Mihaly Karolyi
University Hospital Zurich: UniversitatsSpital Zurich
Matthias Eberhard
University Hospital Zurich: UniversitatsSpital Zurich
Alexander Gotschy
University Hospital Zurich: UniversitatsSpital Zurich
Ioannis Matziris
University Hospital Zurich: UniversitatsSpital Zurich
Hatem Alkadhi
University Hospital Zurich: UniversitatsSpital Zurich
Sebastian Kozerke
University of Zurich: Universitat Zurich
Robert Manka
University Hospital Zurich: UniversitatsSpital Zurich

Research Article

Keywords: cardiac imaging, magnetic resonance imaging, CMR based strain, acute infarction, ischemic myocardial scars

Posted Date: June 11th, 2021

DOI: https://doi.org/10.21203/rs.3.rs-594409/v1

Segmental strain for scar detection in acute myocardial infarcts and in follow-up exams using non-contrast CMR cine sequences

Polacin M[1,3], Karolyi M[1], Eberhard M[1], Gotschy A[2,3], Matziris I[2], Alkadhi H[1], Kozerke S[3], Manka R[1,2,3]

[1] Institute of Diagnostic and Interventional Radiology, University Hospital Zurich, University of Zurich, Raemistrasse 100, 8091 Zurich, Switzerland.
[2] Department of Cardiology, University Heart Center, University Hospital Zurich, University of Zurich, Raemistrasse 100, 8091 Zurich, Switzerland.
[3] Institute for Biomedical Engineering, University and ETH Zurich Gloriastrasse 35, 8092 Zurich, Switzerland.

***Correspondence: Malgorzata Polacin, MD**
University Hospital Zurich,
Raemistrasse 100,
8091 Zurich, Switzerland
E-mail: Malgorzata.Polacin@usz.ch

Abstract

Aims

Scar tissue from myocardial infarction is best visualized with cardiac magnetic resonance (CMR) late gadolinium enhancement (LGE). Gadolinium-free alternatives for detection of myocardial scars are limited. This study investigated the feasibility of myocardial scar detection in acute infarcts and follow-up CMR using non-contrast cine images.

Methods

Fifty-seven patients with acute infarcts (15 female, mean age 61 ± 12 years, CMR 2.8 ± 2 days after infarction) were retrospectively evaluated with follow-up CMR exams available in thirty-two patients (9 female, 35 ± 14 days after infarction). Twenty-eight patients with normal CMR scans (2 female, mean age 47 ± 8 years) served as controls. Global and segmental strain parameters (global peak circumferential [GPCS], global peak longitudinal [GPLS], global peak radial strain [GPRS], segmental peak circumferential [SPCS], segmental peak longitudinal [SPLS], and segmental peak radial strain [SPRS]) were calculated from standard non-contrast balanced SSFP cine sequences using commercially available software (Segment CMR, Medviso, Sweden). Visual assessment of wall motion abnormalities on short axis cine images, as well as segmental circumferential strain calculations (endo-/epicardially contoured short axis cine and resulting polar plot strain map) of every patient (acute imaging and follow-up CMR) were presented for two blinded readers in random order, who were advised to localize potentially infarcted segments, blinded to LGE images and clinical information.

Results

While global strain values were impaired in patients with acute infarcts compared to controls (GPCS p= 0.01; GPLS p= 0.04; GPRS p= 0.01), global strain was similar between first CMR and follow-up imaging in the subgroup of 32 patients (GPCS p= 0.7; GPLS p=0.8; GPRS p=0.2). In acute infarcts and in follow-up CMR, patients had reduced mean SPCS in infarcted segments compared to remote myocardium (acute p= 0.03, follow-up exams p= 0.02).

SPCS values in infarcted areas were similar in acute infarcts and in follow-up exams (p=0.8). In acute infarcts 74.6 % of all in LGE infarcted segments (141/189) were correctly localized in polar plot strain maps compared to 44.4% (84/189) of infarcted segments detected by visual wall motion assessment only ($p < 0.05$). In follow-up exams, 81.5 % of all in LGE infarcted segments (93/114 segments) were correctly localized in polar plot strain maps compared to 51.8 % (59/114) of infarcted segments detected by visual wall motion assessment ($p < 0.05$).

Conclusion

Segmental circumferential strain derived from routinely acquired cine sequences detects nearly 75 % of acute infarcts and about 80% of infarcts in follow-up CMR and can potentially be used for scar identification based on non-contrast cine images, when gadolinium cannot be applied or LGE images are non-diagnostic.

Key Words: cardiac imaging, magnetic resonance imaging, CMR based strain, acute infarction, ischemic myocardial scars

Abbreviations:

AUC	area under the curve
CMR	cardiac magnetic resonance
FT	feature tracking
GPCS	global peak circumferential strain
GPLS	global peak longitudinal strain
GPRS	global peak radial strain
ICC	intraclass correlation coefficient
i.v.	intravenous
LGE	late gadolinium enhancement

LV	left ventricle/left-ventricular
LVEDV	left ventricular end-diastolic volume
LVEF	left ventricular ejection fraction
LVESV	left ventricular end-systolic volume
LVSV	left ventricular stroke volume
MI	myocardial infarction
ms	milliseconds
min	minute(s)
ROC	receiver operating characteristics
s	seconds
SPCS	segmental peak circumferential strain
SPLS	segmental peak longitudinal strain
SPRS	segmental peak radial strain
SSFP	steady- state free precession
T	Tesla
VWMA	Visual wall motion abnormality

Introduction

Upon myocardial infarction (MI), scar tissue is best visualized by cardiac magnetic resonance imaging (CMR) with late gadolinium enhancement (LGE) [1]. Intravenous application of gadolinium-based contrast agents is mandatory before acquiring LGE sequences. However, gadolinium should be used carefully in some patient groups, such as patients with severely reduced kidney function. Recently, alternative methods of scar detection based on routinely acquired cine images have gained attention [2,3], but the underlying studies are mostly in a proof-of-concept stage, require more extensive system integration and are not yet practicable in the clinical setting.

Myocardial deformation during cardiac contraction can be described by vectors in the radial, circumferential and longitudinal directions. Negative strain values are measured for

circumferential and longitudinal direction in normal myocardium, while radial strain provides positive values due to thickening in the radial direction during systole [4]. MI leads to local necrosis of myocytes with scar replacement, consecutively disturbing normal global and segmental strain. Myocardial tagging is the reference standard in CMR for measuring myocardial strain but needs dedicated sequences [5]. Myocardial feature tracking (FT) has been introduced as a novel technique for myocardial strain quantification based on routinely acquired SSFP cine sequences [3,6–8]. Especially FT methods based on non-rigid registration and segmentation, where not only myocardial borders are traced, but the whole image content is tracked throughout the cardiac cycle, seem to detect segmental pathologies in patients after myocardial infarction [9,10]. In this study, global and segmental strain derived from non-contrast cine images was analyzed in patients with acute infarction and in follow-up exams and the feasibility of using segmental strain in infarcted segments for scar detection was investigated.

Methods

Study population

From April 2016 to December 2020 57 patients (15 female, mean age 61 ± 12 years) with acute myocardial infarcts in CMR (imaging 2.8 ± 2 days [0-6 days]) were retrospectively assessed. Thirty-two out of 57 patients had a follow-up CMR (35 ± 14 days, [20-86 days]). Patients with concomitant primary cardiomyopathies (n= 2) or non-diagnostic LGE images (n= 3) were not enrolled. Twenty-eight individuals (2 female, mean age 48 ± 10 years) with normal cardiac MRI examinations during the same time period were also retrospectively included. CMR referrals in the control group were exclusion of structural heart disease (n= 4) or exclusion of coronary artery disease (n=24). This study was conducted in accordance to the Declaration of Helsinki and its later amendments and the institutional review board approved this retrospective study. All participants gave written informed consent. Characteristics of patient groups and controls are shown in Table 1.

CMR data acquisition

CMR data were obtained on a 1.5T MR system (Achieva, Philips Healthcare, Best, the Netherlands) using a dedicated 5-channel phased array coil. Functional and geometric assessment of the left ventricle (LV) was performed using cine balanced steady-state free precession (SSFP) images in standard long-axis geometries (two-, three- and four-chamber view) as well as in short-axis orientation covering the entire LV (field of view: 350 × 350 mm^2, matrix: 300 × 300, repetition time/echo time: 3.0/1.5 ms, in-plane resolution, 1.2 × 1.2 mm^2; number of cardiac phases: 50, section thickness: 8 mm). Edema-sensitive black-blood T2-weighted images with fat saturation in five short-axis slices were acquired for visualizing myocardial edema [11]. LGE images (inversion recovery gradient-echo sequence: field of view: 350 × 350 mm^2; matrix: 234 × 234 repetition time/echo time: 7.4/4.4 ms; inversion time: 205–255 ms; flip angle: 20°; in-plane resolution: 1.5 × 1.5 mm^2; section thickness: 8 mm) covering the entire LV in short axis view as well as in 2-,3- and 4 chamber view were acquired 15

minutes after administration of a bolus of 0.2 mmol gadobutrol (Gadovist; Bayer Schering Pharma, Zurich, Switzerland) per kilogram body weight.

CMR Data analysis

Feature tracking analysis – Global and segmental strain parameters (global peak circumferential [GPCS], global peak longitudinal [GPLS], global peak radial strain [GPRS], segmental peak circumferential [SPCS], segmental peak longitudinal [SPLS], and segmental peak radial strain [SPRS]) were calculated from standard non-contrast balanced SSFP cine sequences using commercially available software (Segment CMR, Medviso, Sweden) in accordance with the American Heart Association`s 16 segment model [9]. Image registration was started separately for the short-axis stack (for calculation of global and segmental circumferential and radial strain) and for the three long axes (needed for global and segmental longitudinal strain). After image registration, endocardium and epicardium of every slice of the short-axis stack (8-12 slices, depending on the length of the LV) and in the 2-,3-,4-chamber long axis were manually contoured in end-diastole and in end-systole and these contours were propagated throughout the cardiac cycle calculating myocardial strain. All FT strain analyses (patients and controls) were performed blinded to patient information and LGE images by one reader (reader A: 5 years of experience in cardiac imaging). Due to the semi-automatic nature of FT analyses, twenty-eight random cases were chosen to perform interobserver agreement (reader B: two years of experience in cardiac imaging), blinded to results of the first reader.

Localization of potentially infarcted segments in circumferential strain calculations and in cine images – Reader A and B were advised to detect potentially infarcted segments in segmental circumferential strain calculations (endo-/epicardially contoured short-axis cine stack with resulting polar plot strain map, *Fig. 1*) as well as in the corresponding short-axis cine images, visually recognizing wall motion abnormalities (VWMA). In both methods, all 16 segments (basal, midventricular and apical section) were evaluated through a cardiac cycle and segments were classified in a binary manner (infarcted or not infarcted). Datasets of patients

(acute imaging and follow-up CMR) and controls were mixed and presented in random order to the readers. Both readers were blinded to each other, to LGE images and to clinical information.

Assessment of infarcted segments in LGE images – In a separate session, both readers had to select affected segments (short axis stack LGE, black-blood T2-weighted images with fat saturation) blinded to clinical information. Reference standard was the existing corresponding report (revised by a cardiologist with over 15 years of experience in CMR). Ventricular volumes and function were calculated using IntelliSpace Portal, performed by reader A (Philips, Version 8.0.3) (*Tab.1*).

Statistical analyses

Statistics were performed using commercially available software (IBM SPSS Statistics, release 25.0; SPSS, Armonk, NY). Categoric data are expressed as numbers or percentages and quantitative data are expressed as means ± standard deviations. Normal distribution was tested by the Kolmogorov–Smirnov test. Two-tailed paired *t*-tests or Wilcoxon signed rank were used to compare global and segmental strain values as well as to compare infarcted segments found in LGE, circumferential strain calculations and by visual wall motion assessment. Interobserver agreement was investigated using the intraclass correlation coefficient (ICC). ICC = 0.50- 0.75 was considered moderate, ICC = 0.75- 0.9 was considered good and ICC > 0.9 was considered excellent agreement [12]. Receiver operating characteristics (ROC) were calculated to determine the cut-offs of segmental strain values and area under the curve (AUC) for segmental circumferential strain in order to differentiate infarcted from remote myocardium. ROC curve analysis was not performed for segmental longitudinal or radial strain due to lacking significance between strain values in infarcted and remote myocardium. Statistical significance was supposed at a p-value below 0.05.

Results

LGE and edema

In patients with acute infarction, 189 out of 896 segments showed LGE (21.1%) and myocardial edema. Myocardial edema was also detected in 27 segments without LGE. Mean scar burden per patient was 23.4% ± 6 (range 8 - 59%) and the average amount of infarcted segments per patient was 3.7 (range: 2-9).

In the subgroup of patients with follow-up exams 118 out of 512 segments showed LGE (23 %). Scar burden at acute imaging timepoint was 25.1% ± 5 per patient (range 12 - 56%) along with myocardial edema, further 10 segments had myocardial edema without concomitant LGE. Scar burden decreased in follow-up exams (20.7 ± 4, range 5 - 48%) (*Tab.1*). No LGE was found in the control group.

Global strain

Mean global strain values were reduced in patients compared to controls (GPCS: -10.3% ± 3 vs. 20.1% ± 2, p = 0.01; GPLS: -10.7 % ± 5 vs. 18.6 % ± 2 p=0.04; GPRS: 27.9% ± 5 vs. 39.2% ± 5; p=0.01, *Fig.1*). Mean global strain was similar between both time points in the subgroup with follow-up CMR (GPCS: -10.6% ± 2 vs. -9.5 % ± 3, p= 0.7; GPLS -10.2 % ± 5 vs. 10.9 % ± 5 p=0.8; GPRS 26.8% ± 6 vs. 29.8% ± 4; p=0.2; *Tab.1*).

Segmental strain

Segmental strain in patients with acute infarction

Mean segmental peak circumferential strain (SPCS) was significantly impaired in infarcted segments (- 2% ± 2) compared to mean SPCS of remote myocardium in patients with acute MI (-10.5% ± 1, p= 0.03) (*Fig. 2*), interobserver agreement was excellent (*Tab.2).* Mean segmental peak longitudinal strain (SPLS) and mean segmental peak radial strain in infarcted segments were mildly impaired (SPLS - 6.5 % ± 8 and SPRS 15.9% ± 7) compared to SPLS and SPRS of remote myocardium (SPLS -11.8% ± 5 and SPRS 23.4% ± 7, p= 0.7

and 0.5) (*Fig.3*). In a blinded comparison, where infarcted segments should be identified by visual assessment of wall motion abnormalities (VWMA) in native cine images and in segmental circumferential strain calculations (based on cine images) (Fig.1), 141 from 189 infarcted segments (74,6%) were considered “infarcted” in circumferential strain calculations and 84 out of 189 in VWMA (44,4%). 30 infarcted segments were not identified in circumferential strain calculations, but all missed segments belonged to patients already diagnosed with potential scars. 15 segments were assumed “infarcted” in circumferential strain calculations without displaying LGE, all those segments had myocardial oedema. No normal segments (without oedema and LGE) in patients nor segments in controls were assumed “infarcted” by VWMA or circumferential strain calculations.

Segmental strain in follow-up MRI

In follow-up exams mean SPCS and SPRS in infarcted segments showed markedly impaired strain values compared to mean SPCS and mean SPRS of remote myocardium (SPCS -2.4% ± 2 vs.-13.4% ± 2, p= 0.02; SPRS 16.7% ± 4 vs. 32.4% ± 3, p= 0.02; *Fig. 3*) with excellent interobserver agreement (*Tab. 2)*. Direct comparison between imaging in the acute setting and in follow-up CMR revealed no significant differences in segmental strain values between infarcted segments and remote myocardium, however, a tendency towards lower segmental circumferential strain of remote myocardium in the acute subgroup was noticeable (acute CMR -10.6% ± 1 vs. follow-up -12.9% ± 2, p= 0.07; Fig.3).

Since segmental circumferential strain appeared to be suitable for identifying segments with ischemic scars, we performed ROC analysis to detect the optimal cut-off values for SPCS for discrimination of scar tissue and remote myocardium (AUC 0,89 [0,878 – 0,923). In our patient group we calculated, that below a SPCS value of -5,9 % (sensitivity of 86,2 %, specificity of 83,5%; [*Fig.4])* segments are considered infarcted.

Localization of potentially infarcted segments based on segmental circumferential strain calculations revealed 93 out of 114 infarcted segments (81,6%). Fifty-nine segments with wall motion abnormalities were found in cine images (51,8%). No false positive findings were

detected in circumferential strain calculations by any reader, however one patient with small subendocardial infarction (1 segment) was missed in segmental circumferential strain calculation.

Discussion

This study analyzed global and segmental strain derived from non-contrast cine images in acute infarcts and follow-up exams and the feasibility of using segmental circumferential strain for detection of ischemic myocardial scars.

Intravenous application of gadolinium-based contrast agents is necessary to perform LGE sequences, the gold standard for scar imaging after MI. However, patients with recent MI may suffer from acute renal failure and application of gadolinium should be used restrictively in those cases. In the clinical setting, established alternatives for scar detection in native CMR sequences are limited. With native T1 mapping, scar and remote myocardium can be differentiated due to different tissue relaxation times [13]. However, additional mapping sequences need to be acquired and to achieve accurate measurements, standardized parameters for healthy myocardium need to be defined separately for every scanner. Moreover, while acute infarcts can be reliably detected in native T1 maps, T1 values of infarcted areas normalize after acute infarction with resulting lower specificity for chronic infarcts [14]. Some artificial intelligence-based techniques successfully detected scar tissue in non-contrast cine CMR sequences [2,15], but these methods are mostly still in a proof-of-concept stage and are not yet practicable in clinical use.

Myocardial feature tracking (FT) was introduced as a novel technique for myocardial strain quantification based on routinely acquired cine sequences. Infarcted tissue leads to altered global and segmental myocardial strain due to reduced contractility of fibroblasts, that gradually replace necrotic myocardium after MI [16]. Impairment of global strain in patients with acute and chronic infarcts have been reported by various studies [17,18]. Accordingly, GPLS, GPRS and especially GPCS was impeded in our patient cohort compared to healthy controls. Studies analyzing segmental strain in patients with infarcts in the last decade

revealed heterogenous results, in particular problems with accuracy and reproducibility of segmental strain values have been reported [19]. Newer algorithms for strain quantification based on non-rigid algorithm for image registration and segmentation with tracking of the whole image content - instead of tracking myocardial borders only- seem to identify scarred myocardium in segmental circumferential strain more sufficiently [10,20,21].

In our patient group, mean SPCS in infarcted tissue was impaired compared to SPCS of remote myocardium and this was observed in both acute imaging as well as in follow-up CMRs; in ROC analyses cut-off value was -5.9%, below which segments were considered infarcted.

Also direct comparison of wall motion and segmental circumferential strain calculations of every patient in a blinded dataset revealed markedly more “infarcted” segments in segmental circumferential strain calculations than by looking at cine images only and this was true for the acute timepoint (74.6% vs. 44.4%) as well as in follow-up exams (81.5% vs. 52 %). Imaging in the early phase after MI is challenging due to complex pathophysiologic processes of the acutely infarcted myocardium and compensatory mechanisms of adjacent remote tissue [22], nevertheless segmental circumferential strain is able to detect nearly 75% of acutely infarcted segments. Although some infarcted segments were not found by segmental circumferential strain calculations, not even one patient with acute infarction was missed and only one patient with small subendocardial scar was missed in the follow-up exam.

In the follow-up exams, we noticed reduced scar burden (25.1 % vs. 20.7%), most probably due to subsided edema [23]. More infarcted segments were detected by VWMA in the follow-up exam (52%) than in the first CMR (44.4%), possibly due to more evident wall motion abnormality as myocardial thinning of infarcts starts in the subacute stage [24]. This transitional stage from acute to subacute infarct did not influence global strain, all global strain values were similar in acute exam and in follow-up CMR. Furthermore, direct comparison of segmental strain values in infarcted segments between both time points showed interchangeable values.

Analyzing values for remote myocardium in acute infarcts, segmental circumferential strain was slightly more impaired compared to remote myocardium in follow-up exams and further

analyses revealed, that edematous segments were mainly responsible for strain impairment, suggesting influence of myocardial edema on segmental circumferential strain.

In summary, segmental circumferential strain based on non-contrast cine images detects most ischemic scars in the acute timepoint and in follow-up exams in contrast to visual evaluation of cine images and can potentially be used for scar identification. Since CMR based strain is increasingly established in clinical use, this method might be a promising problem solver in patients with ischemic heart disease who cannot receive or reject gadolinium or when LGE images are non-diagnostic.

Limitations

Some limitations must be mentioned. This is a small retrospective study of 57 patients with follow-up CMR exams of 32 -mostly male- patients and possible gender differences were not taken into account. The mean interval of 5 weeks between initial imaging and follow-up CMR is presumably not long enough to measure remodelling, because of still ongoing pathophysiologic processes and distant time points should be investigated for that matter in further studies.

Segmental circumferential strain calculations derived from short axis cine images use the 16 AHA segment model, so infarction of the apex (segment 17) cannot be diagnosed in SPCS calculations.

Although definition of scar transmurality is important in clinical setting, transmurality assessment in acutely infarcted myocardium might be challenging and was not performed in our study.

Finally, we analyzed global and segmental strain with only one software. Recent studies show, that strain values are not interchangeable between different vendors, thus vendor-specific threshold values need to be defined for infarcted and remote myocardium [10].

Conclusion

Segmental circumferential strain derived from routinely acquired cine sequences detects nearly 75 % of acute infarcts and about 80% of infarcts in follow-up CMR in contrast to visual evaluation of cine images alone and can potentially be used for scar identification, when only native cine sequences are available. Since CMR based strain is increasingly established in clinical use, this method might be a promising approach in patients with ischemic heart disease who cannot receive or reject gadolinium or when LGE images are non-diagnostic.

Author contribution

M.P. and R.M. designed the study. M.P., M.K., A.G. and I.M. provided patient data and images. M.P. and M.K. performed data analysis. M.P. wrote the manuscript. M.E., H.A., S.K. and R.M. proofread the manuscript.

Conflicts of interest

None of the authors of this manuscript has declared any conflict of interest.

References

[1] Treibel TA, White SK, Moon JC. Myocardial Tissue Characterization: Histological and Pathophysiological Correlation. Curr Cardiovasc Imaging Rep 2014;7:1–9. https://doi.org/10.1007/s12410-013-9254-9.

[2] Baessler B, Mannil M, Oebel S, Maintz D, Alkadhi H, Manka R. Subacute and chronic left ventricular myocardial scar: Accuracy of texture analysis on nonenhanced cine MR images. Radiology 2018. https://doi.org/10.1148/radiol.2017170213.

[3] Mangion K, McComb C, Auger DA, Epstein FH, Berry C. Magnetic resonance imaging of myocardial strain after acute st-segment-elevation myocardial infarction a systematic review. Circ Cardiovasc Imaging 2017. https://doi.org/10.1161/CIRCIMAGING.117.006498.

[4] Claus P, Omar AMS, Pedrizzetti G, Sengupta PP, Nagel E. Tissue Tracking Technology for Assessing Cardiac Mechanics: Principles, Normal Values, and Clinical Applications. JACC Cardiovasc Imaging 2015. https://doi.org/10.1016/j.jcmg.2015.11.001.

[5] Rutz AK, Manka R, Kozerke S, Roas S, Boesiger P, Schwitter J. Left ventricular dyssynchrony in patients with left bundle branch block and patients after myocardial infarction: Integration of mechanics and viability by cardiac magnetic resonance. Eur Heart J 2009;30:2117–27. https://doi.org/10.1093/eurheartj/ehp212.

[6] Pedrizzetti G, Claus P, Kilner PJ, Nagel E. Principles of cardiovascular magnetic resonance feature tracking and echocardiographic speckle tracking for informed clinical use. J Cardiovasc Magn Reson 2016. https://doi.org/10.1186/s12968-016-0269-7.

[7] Almutairi HM, Boubertakh R, Miquel ME, Petersen SE. Myocardial deformation assessment using cardiovascular magnetic resonance-feature tracking technique. Br J Radiol 2017. https://doi.org/10.1259/bjr.20170072.

[8] Gastl M, Gotschy A, Polacin M, Vishnevskiy V, Meyer D, Sokolska J, et al. Determinants of myocardial function characterized by CMR-derived strain parameters in left ventricular non-compaction cardiomyopathy. Sci Rep 2019. https://doi.org/10.1038/s41598-019-52161-1.

[9] Morais P, Marchi A, Bogaert JA, Dresselaers T, Heyde B, D'Hooge J, et al. Cardiovascular magnetic resonance myocardial feature tracking using a non-rigid, elastic image registration algorithm: assessment of variability in a real-life clinical setting. J Cardiovasc Magn Reson 2017. https://doi.org/10.1186/s12968-017-0333-y.

[10] Dobrovie M, Barreiro-Pérez M, Curione D, Symons R, Claus P, Voigt JU, et al. Inter-

vendor reproducibility and accuracy of segmental left ventricular strain measurements using CMR feature tracking. Eur Radiol 2019;29:6846–57. https://doi.org/10.1007/s00330-019-06315-4.

[11] Simonetti OP, Finn JP, White RD, Laub G, Henry DA. “Black blood” T2-weighted inversion-recovery MR imaging of the heart. Radiology 1996. https://doi.org/10.1148/radiology.199.1.8633172.

[12] Koo TK, Li MY. A Guideline of Selecting and Reporting Intraclass Correlation Coefficients for Reliability Research. J Chiropr Med 2016. https://doi.org/10.1016/j.jcm.2016.02.012.

[13] Taylor AJ, Salerno M, Dharmakumar R, Jerosch-Herold M. T1 Mapping Basic Techniques and Clinical Applications. JACC Cardiovasc Imaging 2016. https://doi.org/10.1016/j.jcmg.2015.11.005.

[14] O H-Ici D, Jeuthe S, Al-Wakeel N, Berger F, Kuehne T, Kozerke S, et al. T1 mapping in ischaemic heart disease. Eur Heart J Cardiovasc Imaging 2014. https://doi.org/10.1093/ehjci/jeu024.

[15] Zhang N, Yang G, Gao Z, Xu C, Zhang Y, Shi R, et al. Deep learning for diagnosis of chronic myocardial infarction on nonenhanced cardiac cine MRI. Radiology 2019. https://doi.org/10.1148/radiol.2019182304.

[16] Richardson WJ, Clarke SA, Alexander Quinn T, Holmes JW. Physiological implications of myocardial scar structure. Compr Physiol 2015. https://doi.org/10.1002/cphy.c140067.

[17] Reindl M, Tiller C, Holzknecht M, Lechner I, Beck A, Plappert D, et al. Prognostic Implications of Global Longitudinal Strain by Feature-Tracking Cardiac Magnetic Resonance in ST-Elevation Myocardial Infarction. Circ Cardiovasc Imaging 2019. https://doi.org/10.1161/CIRCIMAGING.119.009404.

[18] Nucifora G, Muser D, Tioni C, Shah R, Selvanayagam JB. Prognostic value of myocardial deformation imaging by cardiac magnetic resonance feature-tracking in patients with a first ST-segment elevation myocardial infarction. Int J Cardiol 2018.

https://doi.org/10.1016/j.ijcard.2018.05.082.

[19] Ogawa R, Kido T, Nakamura M, Kido T, Kurata A, Miyagawa M, et al. Diagnostic capability of feature-tracking cardiovascular magnetic resonance to detect infarcted segments: a comparison with tagged magnetic resonance and wall thickening analysis. Clin Radiol 2017. https://doi.org/10.1016/j.crad.2017.05.010.

[20] Zou Q, Zheng T, Zhou SL, Tang XP, Li SH, Zhou W, et al. Quantitative evaluation of myocardial strain after myocardial infarction with cardiovascular magnetic resonance tissue-tracking imaging. Int Heart J 2020;61:429–36. https://doi.org/10.1536/ihj.19-384.

[21] Tantawy SW, Mohammad SA, Osman AM, El Mozy W, Ibrahim AS. Strain analysis using feature tracking cardiac magnetic resonance (FT-CMR) in the assessment of myocardial viability in chronic ischemic patients. Int J Cardiovasc Imaging 2020. https://doi.org/10.1007/s10554-020-02018-w.

[22] Masci PG, Bogaert J. Post myocardial infarction of the left ventricle: the course ahead seen by cardiac MRI. Cardiovasc Diagn Ther 2012. https://doi.org/10.3978/j.issn.2223-3652.2012.04.06.

[23] Rajiah P, Desai MY, Kwon D, Flamm SD. MR imaging of myocardial infarction. Radiographics 2013;33:1383–412. https://doi.org/10.1148/rg.335125722.

[24] Mercado MG, Smith DK, McConnon ML. Myocardial infarction: Management of the subacute period. Am Fam Physician 2013.

Figures & Figure legends

Figure 1a

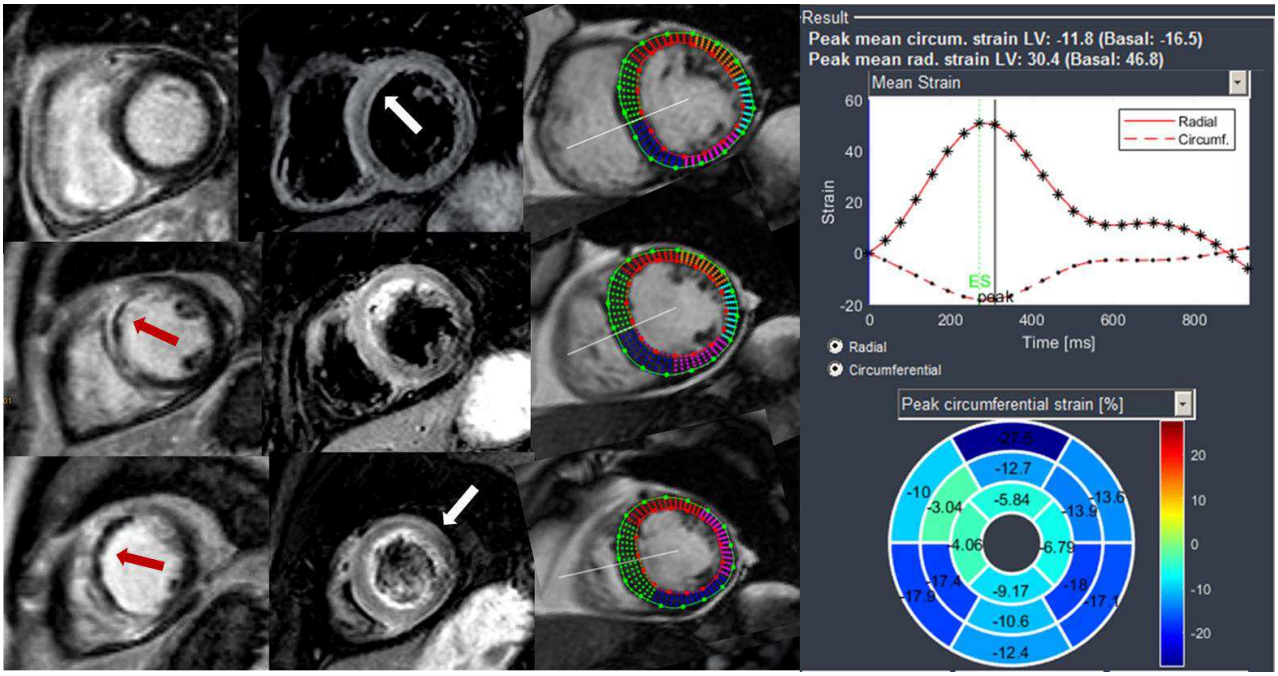

Fig.1a – 48 year old patient with RIVA infarction (2 days after acute infarction)

Left column: LGE in segment 8, 13,14 (red arrows); middle column: concomitant edema extends additionally into segments 2,7,16 (white arrows). Right colum: Endo- and epicardially contoured basal, midventricular and apical cine short axis slices prepared for circumferential strain calculations with polar plot strain map.

Figure 1b

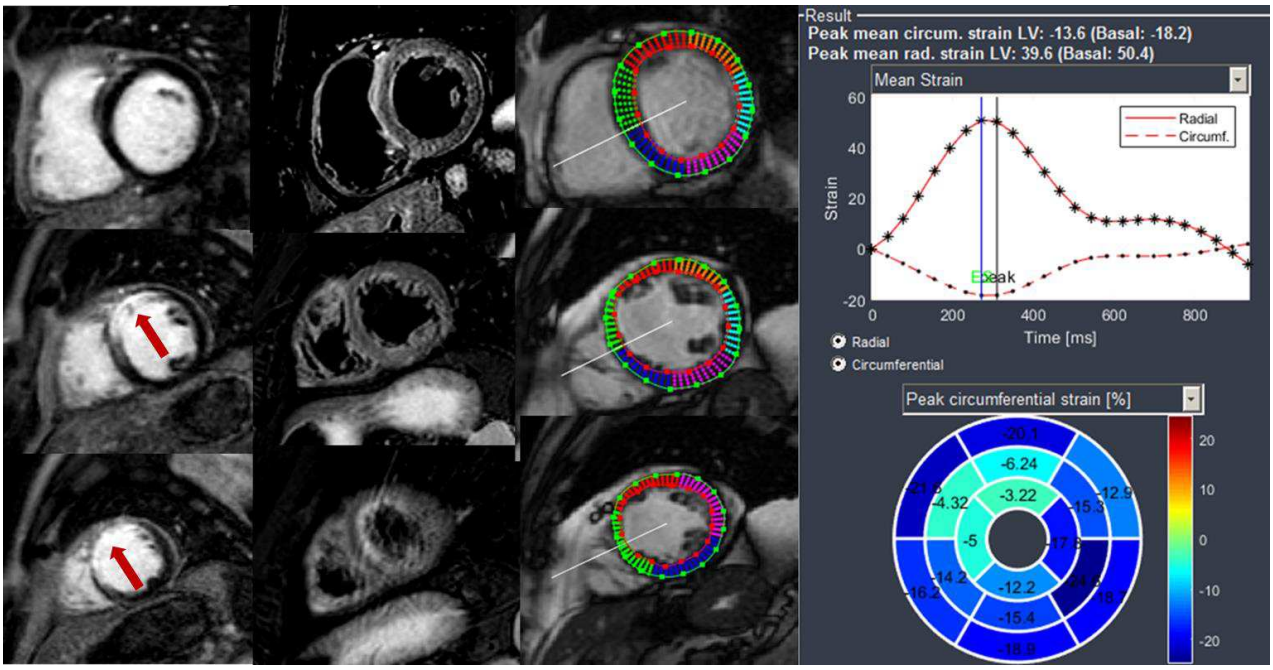

Fig.1b – 48 year old patient with RIVA infarction (35 days after acute infarction)

Left column: LGE in segment 8, 13,14 (red arrows); middle column: no concomitant edema; right colum: Endo- and epicardially contoured basal, midventricular and apical cine short axis slices prepared for circumferential strain calculations with polar plot strain map.

Figure 2

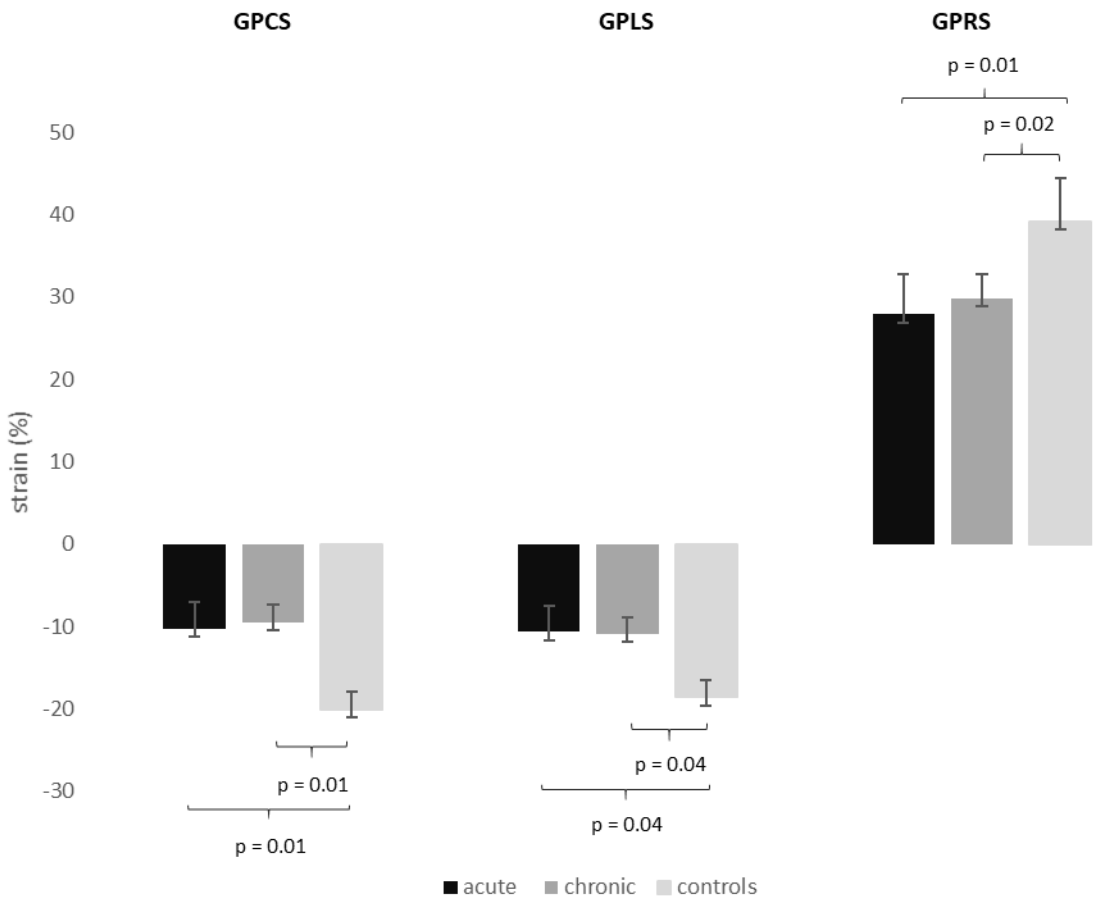

Fig.2– Global strain values in patients and healthy controls

While GPCS, GPLS and GPRS values were very similar comparing both imaging time points, they were significantly impaired compared to healthy controls.

GPCS = global peak circumferential strain, GPLS = global peak longitudinal strain, GPRS = global peak radial strain

Figure 3

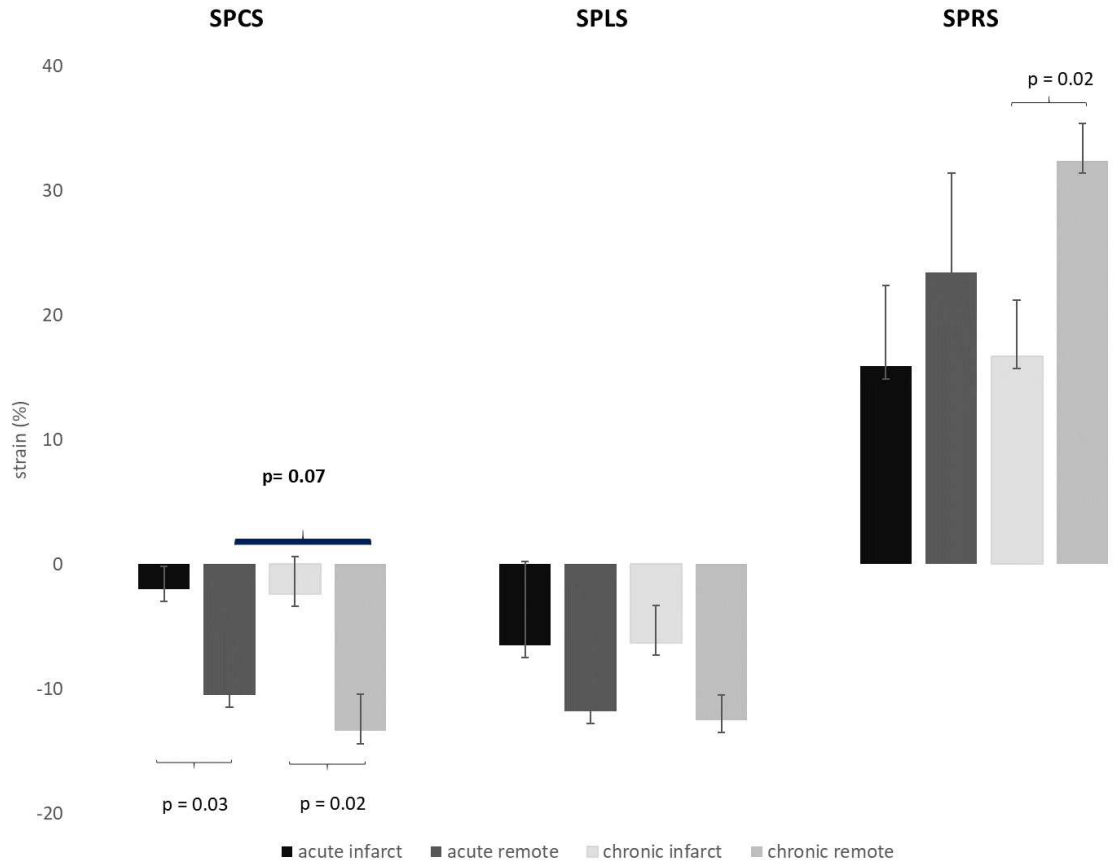

Fig.3 – Segmental strain values for scar tissue and remote myocardium in acute and follow-up CMR

Significantly different values between infarcted and remote myocardium can be detected in SPCS for both imaging time points as well as in SPRS in the follow-up exams.

SPCS = segmental peak circumferential strain, SPLS = segmental peak longitudinal strain, SPRS = segmental peak radial strain

Figure 4

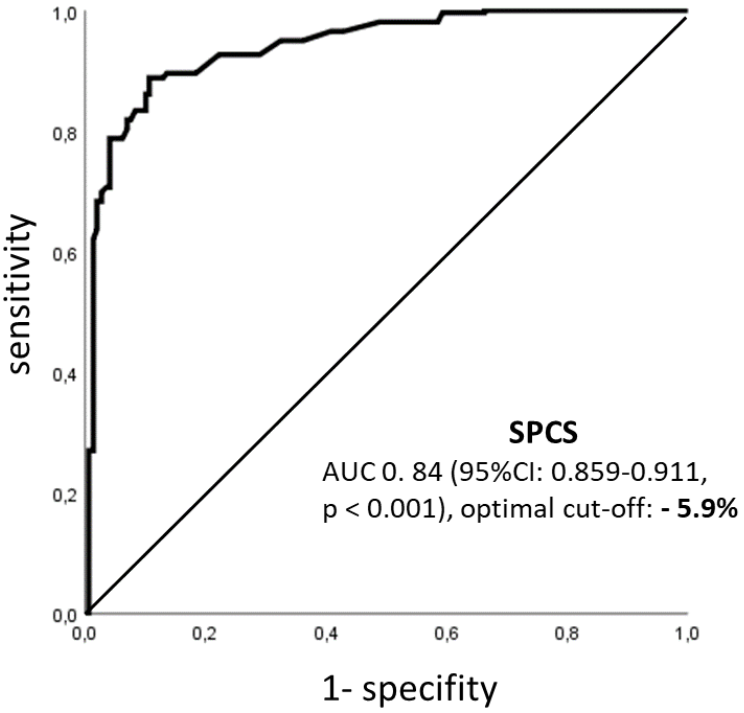

Fig.4 – ROC curve for distinguishing infarcted and remote myocardium based on strain parameters

Below a SPCS value of -5,9 % (sensitivity of 86,2 %, specificity of 83,5%) segments are considered infarcted. ROC= Receiver operating characteristic, SPCS= segmental peak circumferential strain

Figure 4

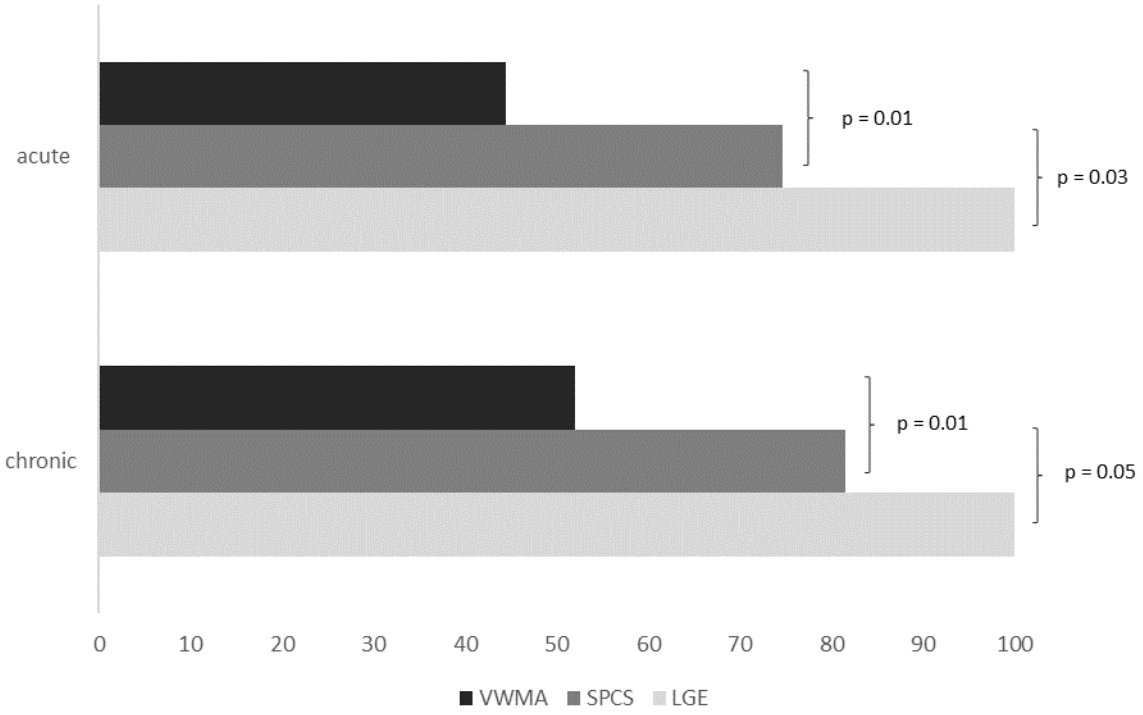

Fig. 5 Localization of infarcted segments showed in segmental circumferential strain calculations

Segmental strain calculations showed significantly more infarcted segments than visual assessment of wall motion abnormalities in cine images and this was significant in both imaging time points.

In follow-up exams more infarcted segments were found in visual assessment of wall motion compared to acute infarcts (52% vs. 44.4%).

LGE = late gadolinium enhancement, SPCS = segmental peak circumferential strain, VWMA = visual wall motion assessment

Tables

Table 1 – Demographic characteristics: patients vs. controls

	acute infarcts (n=57)	controls (n=28)	p-values	acute infarcts	follow-up	p-values
Patient demographics				n= 32		
Sex (male/female)	42/15	26/2		23/9		
Age (years)	61± 12 [35-83]	47 ± 8 [44-69]	0.2	52 ± 7 [35-66]		
Height (m)	1.69 ± 12 [1.68-1.94]	1.65 ± 15 [1.57-1.9]	0.3	1.71 ± 8 [1.68-1.8]		
Weight (kg)	79.8 ± 15 [68-103]	76.4 ± 10 [68-94]	0.7	77.2 ± 11 [68-90]		
BMI	27 +/- 5 [25-31]	25 ± 3 [22-30]	0.5	27 +/- 4 [24-29]		
Left ventricular morphology						
LVEDV (ml,117-200)	191 ± 23 [104-291]	166 ± 37 [81-215]	0.1	172 ± 19 [114-211]	184 ± 27 [145-288]	0.2
LVESV (ml, 31-76)	81 ± 32 [45-195]	87 ± 24 [31-110]	0.4	80 ± 29 [38-160]	86 ± 26 [49-195]	0.8
LVSV (ml, 77-133)	83 ± 15 [57-101]	90 ± 17 [60-111]	0.6	89 ± 18 [57-115]	72 ± 18 [59-103]	0.5
LVEF (%, > 52)	50 ± 8 [28-62]	57 ± 4 [54-69]	0.4	47 ± 10 [50-62]	51 ± 8 [18-49]	0.2
LV Mass (g, 51-87)	60 ±14 [31-95]	52± 8 [37-90]	0.5	60 ±10 [37-95]	53 ± 8 [37-91]	0.6
Global strain						
GPCS (%)	-10.3 +/- 3	- 20.1 +/- 2	0.01	-10.6 +/- 2	- 9,5 +/- 3	0.7
GPLS (%)	-10.7 +/- 5	- 18.6+/- 2	0.04	-10.2 +/- 5	-10.9 +/- 5	0.8
GPRS (%)	27.9 +/- 5	39.2 +/- 5	0.01	26.8 +/- 6	29.8 +/- 4	0.2
Infarcts						
Infarcted segments	189/896	0	-	118/512	118/512	-
Scar burden (%)	23.4 ± 6 [8-59]	0	-	25.1 ± 5 [12-56]	20.7 ± 4 [5-48]	0.6
Myocardial oedema only	27	0	-	10	0	-

BMI= body mass index, *LVEDV*= left ventricular end-diastolic volume, *LVESV*= left ventricular end-systolic volume, *LVSV*= left ventricular stroke volume, *LVEF*= left ventricular ejection fraction; GPCS/GPLS/GPRS = global circumferential/longitudinal/radial strain; values in round brackets are standard, cohort specific LV values; values in square brackets represent the value range

578 **Table 2 – Interobserver agreement**

	ICC acute	ICC chronic
Global strain		
GPCS	0.902 [95% CI:0.878-0.930]	0.916 [95% CI:0.882-0.941]
GPLS	0.850 [95% CI:0.817-0.879]	0.878 [95% CI:0.804-0.929]
GPRS	0.893 [95% CI:0.851-0.939]	0.897 [95% CI:0.878-0.947]
Segmental strain		
SPCS	0.899 [95% CI:0.862-0.922]	0.903 [95% CI:0.869-0.934]
SPLS	0.732 [95% CI:0.711-0.749]	0.719 [95% CI:0.701-0.747]
SPRS	0.804 [95% CI:0.793-0.869]	0.817 [95% CI:0.797-0.902]

579
580
581 *GPCS/GPLS/GPRS = global circumferential/longitudinal/radial strain; SPCS/SPLS/SPRS= segmental*
582 *circumferential/longitudinal/radial strain, ICC = intraclass correlation coefficient*
583 *.*

Figures

Figure 1a

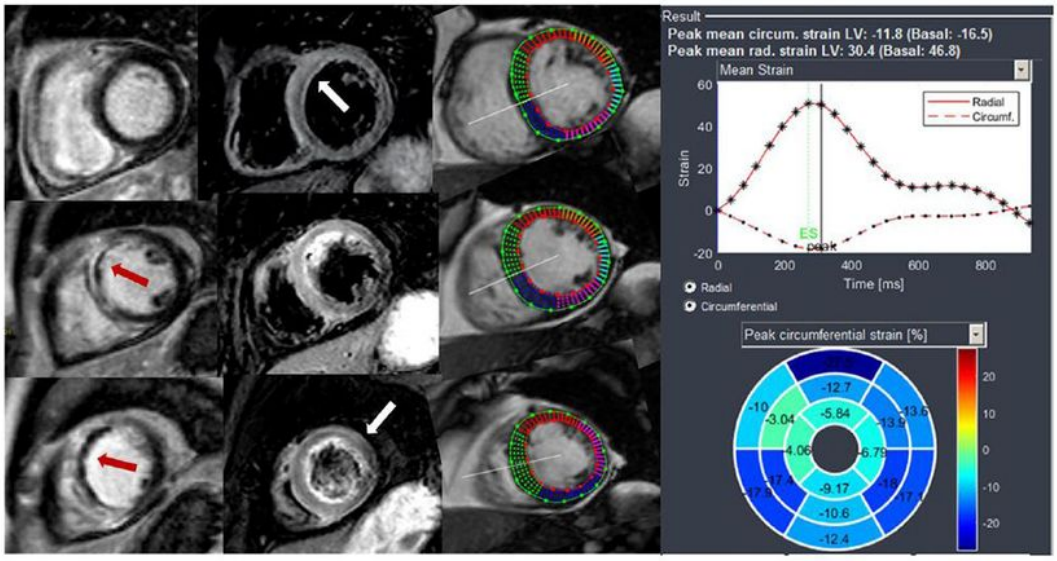

Figure 1b

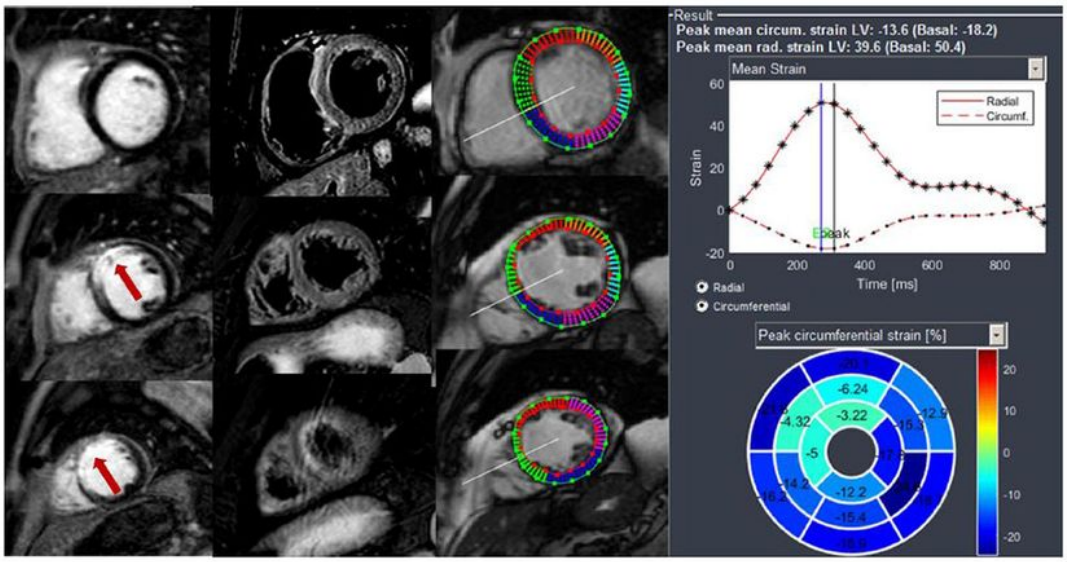

Figure 1

1a – 48 year old patient with RIVA infarction (2 days after acute infarction) Left column: LGE in segment 8, 13,14 (red arrows); middle column: concomitant edema extends additionally into segments 2,7,16 (white arrows). Right colum: Endo- and epicardially contoured basal, midventricular and apical cine short

axis slices prepared for circumferential strain calculations with polar plot strain map. 1b –48 year old patient with RIVA infarction (35 days after acute infarction) Left column: LGE in segment 8, 13,14 (red arrows); middle column: no concomitant edema; right colum: Endo- and epicardially contoured basal, midventricular and apical cine short axis slices prepared for circumferential strain calculations with polar plot strain map.

Figure 2

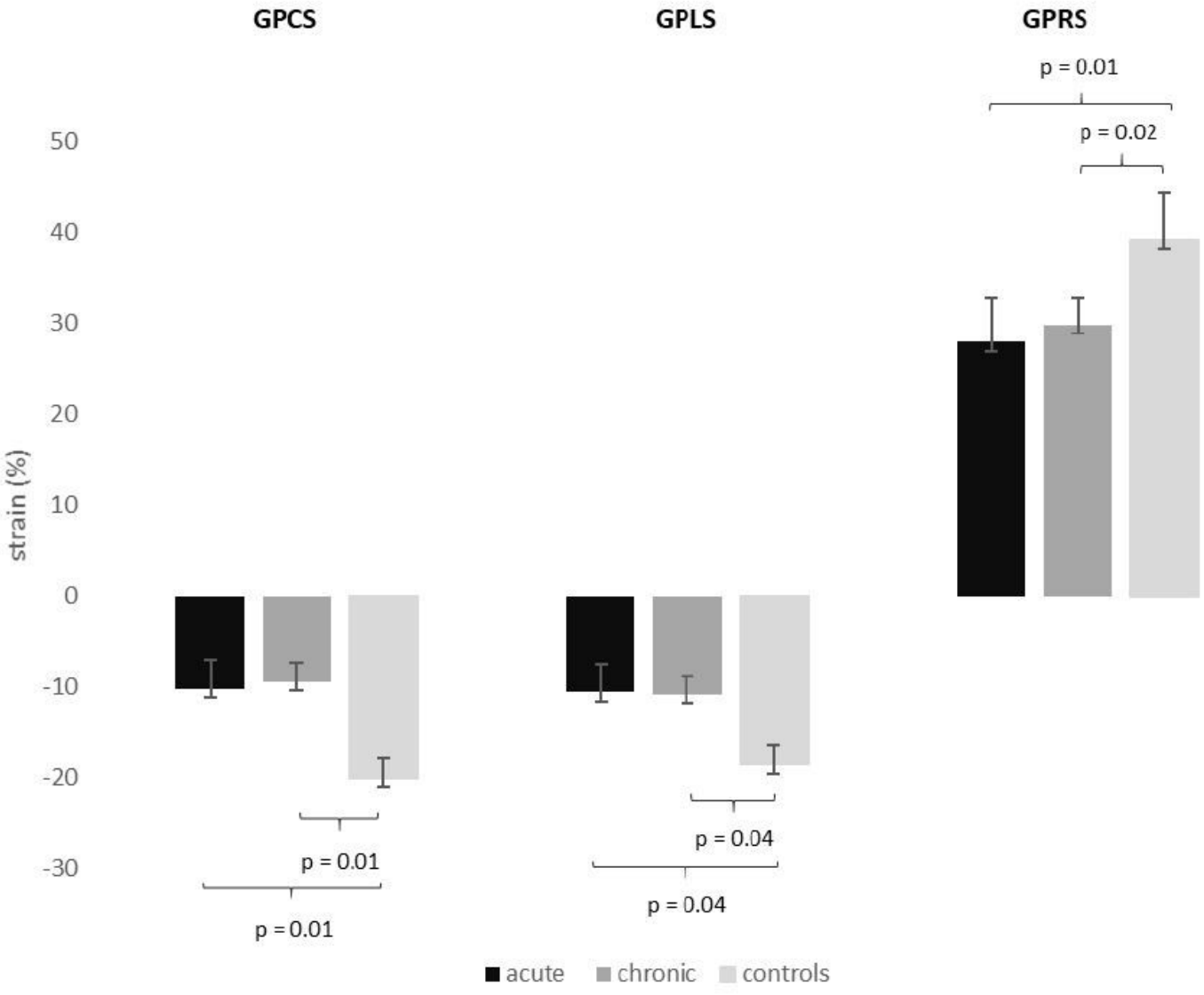

Figure 2

Global strain values in patients and healthy controls While GPCS, GPLS and GPRS values were very similar comparing both imaging time points, they were significantly impaired compared to healthy controls. GPCS = global peak circumferential strain, GPLS = global peak longitudinal strain, GPRS = global peak radial strain

Figure 3

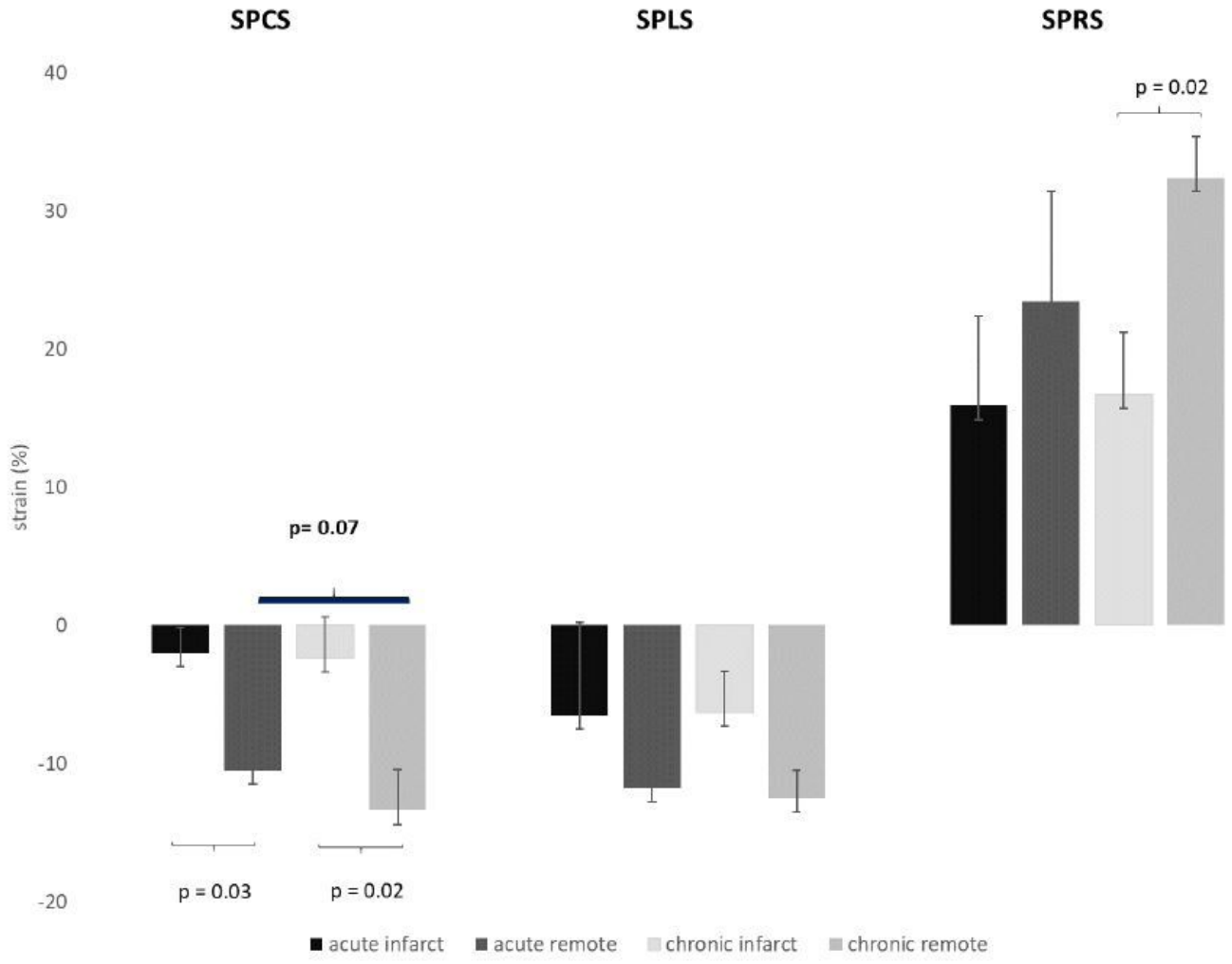

Figure 3

Segmental strain values for scar tissue and remote myocardium in acute and follow-up CMR Significantly different values between infarcted and remote myocardium can be detected in SPCS for both imaging time points as well as in SPRS in the follow-up exams. SPCS = segmental peak circumferential strain, SPLS = segmental peak longitudinal strain, SPRS = segmental peak radial strain

Figure 4

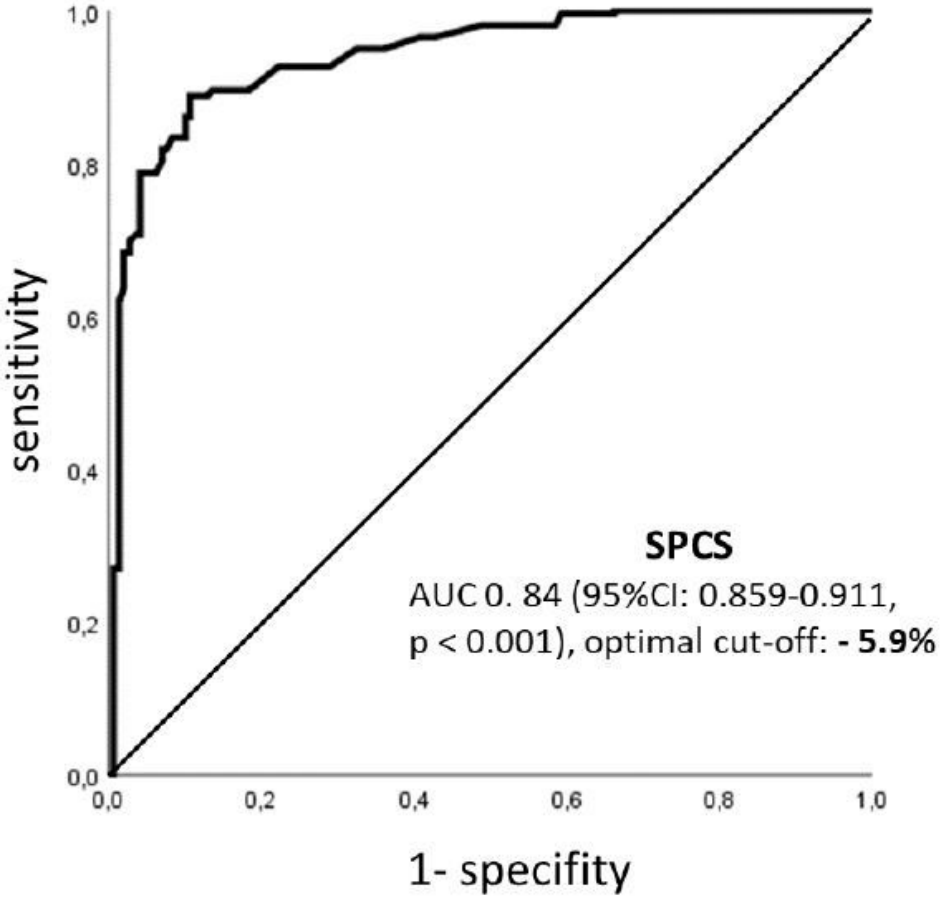

Figure 4

ROC curve for distinguishing infarcted and remote myocardium based on strain parameters Below a SPCS value of -5,9 % (sensitivity of 86,2 %, specificity of 83,5%) segments are considered infarcted. ROC= Receiver operating characteristic, SPCS= segmental peak circumferential strain

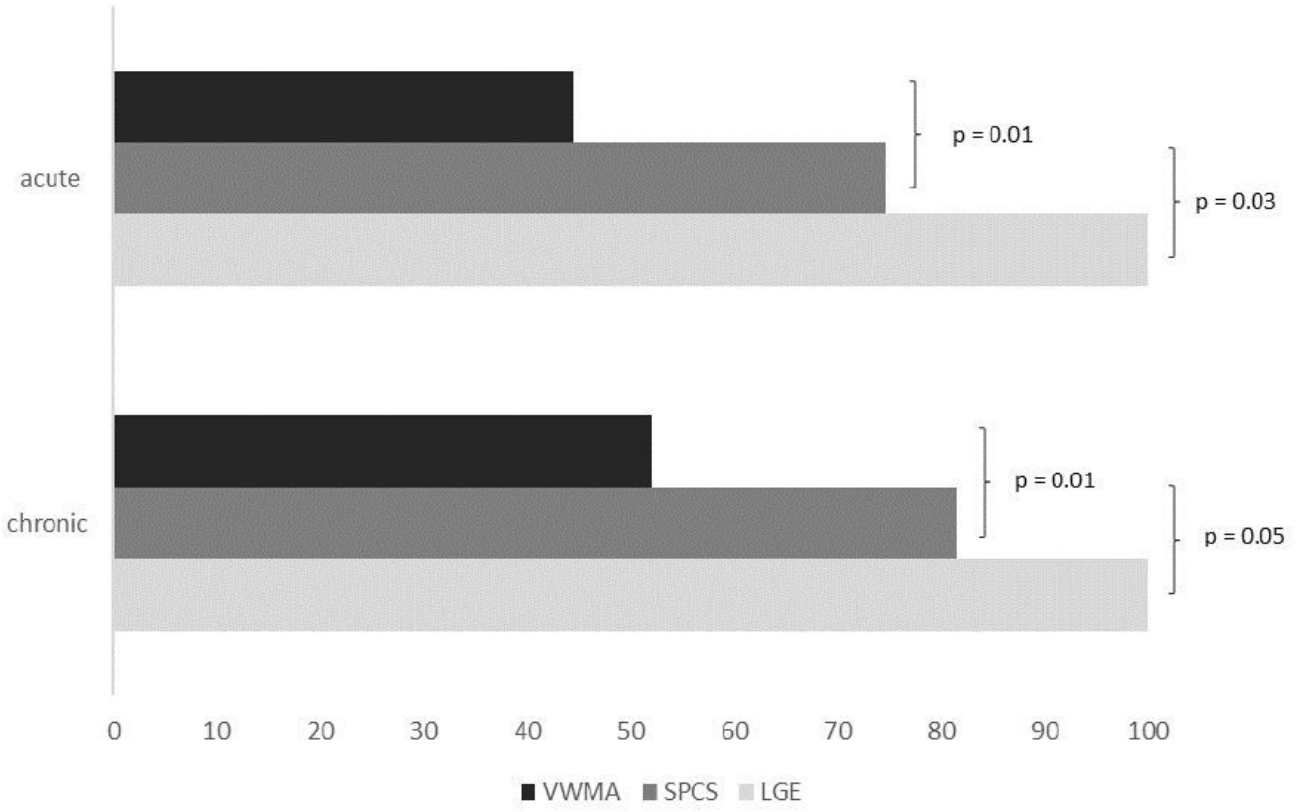

Figure 5

Localization of infarcted segments showed in segmental circumferential strain 548 calculations Segmental strain calculations showed significantly more infarcted segments than visual assessment of wall motion abnormalities in cine images and this was significant in both imaging time points. In follow-up exams more infarcted segments were found in visual assessment of wall motion compared to acute infarcts (52% vs. 44.4%). LGE = late gadolinium enhancement, SPCS = segmental peak circumferential strain, VWMA = visual wall motion assessment